

A computational macroscale model for the time fractional poroelasticity problem in fractured and heterogeneous media

Aleksei Tyrylgin ^{*} Maria Vasilyeva [†] Anatoly Alikhanov [‡] Dongwoo Sheen [§]

Abstract

In this work, we introduce a time memory formalism in poroelasticity model that couples the pressure and displacement. We assume this multiphysics process occurs in multicontinuum media. The mathematical model contains a coupled system of equations for pressures in each continuum and elasticity equations for displacements of the medium. We assume that the temporal dynamics is governed by fractional derivatives following some works in the literature. We derive an implicit finite difference approximation for time discretization based on the Caputo's time fractional derivative. A Discrete Fracture Model (DFM) is used to model fluid flow through fractures and treat the complex network of fractures. We assume different fractional powers in fractures and matrix due to slow and fast dynamics. We develop a coarse grid approximation based on the Generalized Multiscale Finite Element Method (GMsFEM), where we solve local spectral problems for construction of the multiscale basis functions. We present numerical results for the two-dimensional model problems in fractured heterogeneous porous media. We investigate error analysis between reference (fine-scale) solution and multiscale solution with different numbers of multiscale basis functions. The results show that the proposed method can provide good accuracy on a coarse grid.

1 Introduction

Recently, various applications of differential equations with fractional order derivatives have been of increasing interest. Moreover, in contrast to the classical derivative of integer order, there are many non-identical definitions of derivatives of fractional order [17, 22, 19]. For example, fractional derivative is used in models of viscoelastic bodies, continuous media, transformation of temperature, humidity in atmospheric layers, diffusion equations, and in other areas [31, 33, 46, 25, 41]. In addition, in the middle of the twentieth century F. Mainardi and M. Caputo showed that the use of differential equations with fractional derivatives more better the models of thermoviscoelasticity are described, which make it possible to more accurately reproduce the experimentally observed data [12, 11, 35, 36]. The relevance of such a study is explained by the fact that the use of a rich arsenal of fractional differentiation methods will make new methods for statistical analysis of nonstationary time series.

In this paper, we study a fractional poroelasticity model. The basic mathematical structure of the poroelasticity models are usually coupled equations for pressure and displacement. In their modern form, such models were proposed in the works of M. Biot [7, 8, 14, 20, 27]. Biot's model describes the coupled processes of deformation of the elastic medium and the flow of fluid. The model is macroscopic in the sense that the space containing the poroelastic medium is filled with a two-phase medium, with one phase corresponding directly to the porous medium, and the second to the fluid contained in the pores [34, 24].

^{*}Laboratory of Computational Technologies for Modeling Multiphysical and Multiscale Permafrost Processes, North-Eastern Federal University, Yakutsk, Republic of Sakha (Yakutia), 677980, Russia & North-Caucasus Center for Mathematical Research, North-Caucasus Federal University, Stavropol, 355017, Russia.

[†]Department of Mathematics and Statistics, Texas A&M University, Corpus Christi, 78412, Texas, USA. Email: maria.vasilyeva@tamucc.edu.

[‡]North-Caucasus Center for Mathematical Research, North-Caucasus Federal University, Stavropol, 355017, Russia. Email: aaalikhonov@gmail.com.

[§]Department of Mathematics, Seoul National University, Seoul 08826, South Korea. Email: dongwoosheen@gmail.com.

In our case, we consider mathematical models for flow in the multicontinuum media, which describes complex flow processes in multiscale fractured heterogeneous porous media [15, 16, 2, 3, 1]. The flow in fractures has a significant impact on filtration processes and requires careful consideration [28, 29]. Since the fractures are characterized by high permeability and their thickness is significantly smaller than the size of the simulated field, this leads to the need to build special mathematical models of multicontinuum, where independent variables are distinguished to describe the flow in a porous medium and in the network of fractures taking into account the special flow function [3, 26, 30].

The extension of the poroelasticity to include fractional time derivatives appeared in earlier works [4, 13, 32, 18], where physical motivations are presented. The fractional time derivatives represent the memory effects that occur in porous media flows. One way to account for them is to introduce fractional time derivatives. The main distinction of our model from previous models consists of several points. First, we use different fractional time derivatives for each continua as each continua can have different propagation dynamics, and thus, different memory terms. Secondly, we assume that the media have multiple spatial scales, which commonly occur in porous media applications. Our main goal is to derive a computational macroscopic model for fractional Biot's system in multicontinuum heterogeneous media.

Our computational macroscale model is based on the Generalized Multiscale Finite Element method (GMsFEM). The GMsFEM has been studied for a various applications related to poroelasticity problems [9, 10, 3, 40]. The multiscale finite volume method has been applied for the simulation of the flow problems in fractured porous media [23, 39]. For the effective numerical solution of such problems different homogenization techniques have been developed [30, 29, 5, 37, 6, 21]. Mathematical models of the flow problems in fractured porous media using the GMsFEM have been researched [45, 42, 38, 2]. The GMsFEM and NLMC approach for solution of the flow problems in multicontinuum media have been generalized in [42, 44, 43].

In this paper, we consider the GMsFEM for the poroelasticity problems in multicontinuum media with the fractional order time derivative. For temporal discretization, we use a finite different approximation, which has a memory term. Since our model equation has multiple fractional powers, there multiple unknowns with memory effects. Because the media properties have multiple scales, we use multiscale basis functions to reduce the dimension of the problem. The multiscale basis functions are constructed for flow and mechanics. Construction of the basis functions for flow problem in multicontinuum media is based on the solution of the coupled system of equations in each local domains. In each coarse grid block, we compute the snapshots by solving local problems for pressures in multicontinuum media and displacement. Taking the corresponding to the dominant eigenvalues, and multiplying by a multiscale partition of unity, we can construct our multiscale basis functions.

Numerical results are presented. In our numerical examples, we consider two different type of media. In the first case, we have one continuum. In the second example, we have two continuum, which increases the number of equations. The memory term is handled by saving solution snapshots. Because the solution is on the coarse grid, this saves some computational time. We consider numerical simulations using different number of basis functions. In all examples, when we increase the number of basis functions, the error decreases. In particular, using fewer basis functions, we obtain accurate solution approximation.

The work is organized as follows. In Section 2, we present the mathematical model of the poroelasticity problem in multicontinuum medium. Then in Section 3, a fine grid approximation is constructed using the finite element method and the fractional-order derivative. In Section 4, we present a coarse grid approximation using the Generalized Multiscale Finite Element method, where we describe the construction of the multiscale basis functions and coarse grid system construction. Numerical results for two-dimensional model poroelasticity problems are presented in Section 5. Finally, we present conclusions.

2 Problem formulation

The time fractional flow in porous media $\Omega \subset R^d$ can be described by the following equation

$$c \frac{\partial^\alpha p}{\partial t^\alpha} - \nabla \cdot (k \nabla p) = 0, \quad \Omega \times (0, T), \quad (1)$$

where $k = \frac{\kappa}{\mu}$ with the permeability k and the fluid viscosity μ , and

$$\partial_t^\alpha p(t) = \frac{1}{\Gamma(1-\alpha)} \int_0^t (t-s)^{-\alpha} \frac{\partial p}{\partial s}(s) ds, \quad 0 < \alpha \leq 1, \quad (2)$$

denotes the Caputo derivative of the order α .

To consider flow in fractured porous media, we denote $\gamma \subset R^{d-1}$ as a computational domain for low dimensional fracture networks model. Therefore, we have the following system of equations for flow in fractured porous media:

$$\begin{aligned} c_m \frac{\partial^{\alpha_m} p_m}{\partial t^{\alpha_m}} - \nabla \cdot (k_m \nabla p_m) + \eta_{mf}(p_m - p_f) &= 0, \quad \Omega \times (0, T), \\ c_f \frac{\partial^{\alpha_f} p_f}{\partial t^{\alpha_f}} - \nabla \cdot (k_f \nabla p_f) + \eta_{mf}(p_f - p_m) &= 0, \quad \gamma \times (0, T), \end{aligned} \quad (3)$$

where p_m and p_f are the pressure in porous matrix and fractures, κ_m and κ_f the porous matrix and fractures permeability ($k_m = \frac{\kappa_m}{\mu}$ and $k_f = \frac{\kappa_f}{\mu}$), and η_{mf} the mass transfer term between the porous matrix and fractures.

We can write a similar system of equations for flow in triple continuum approach, where the first continuum describe a flow in the matrix of the porous media, the second continuum belongs to the network of small highly connected fracture network (natural fractures) and the third continuum related to the flow in low dimensional fracture networks (large-scale fractures). We have following system of equations for (p_1, p_2, p_f) :

$$\begin{aligned} c_1 \frac{\partial^{\alpha_1} p_1}{\partial t^{\alpha_1}} - \nabla \cdot (k_1 \nabla p_1) + \eta_{12}(p_1 - p_2) + \eta_{1f}(p_1 - p_f) &= 0, \quad \Omega \times (0, T), \\ c_2 \frac{\partial^{\alpha_2} p_2}{\partial t^{\alpha_2}} - \nabla \cdot (k_2 \nabla p_2) + \eta_{12}(p_2 - p_1) + \eta_{2f}(p_2 - p_f) &= 0, \quad \Omega \times (0, T), \\ c_f \frac{\partial^{\alpha_f} p_f}{\partial t^{\alpha_f}} - \nabla \cdot (k_f \nabla p_f) + \eta_{1f}(p_f - p_1) + \eta_{2f}(p_f - p_2) &= 0, \quad \gamma \times (0, T), \end{aligned} \quad (4)$$

where, for the continuum index $i = 1, 2, f$, p_i denotes the pressure, κ_i the permeability ($k_i = \frac{\kappa_i}{\mu}$, μ the fluid viscosity), and η_{ij} the mass transfer term that are proportional to the continuum permeabilities.

We can generalize it as flow model for multicontinuum media

$$c_i \frac{\partial^{\alpha_i} p_i}{\partial t^{\alpha_i}} - \nabla \cdot (k_i \nabla p_i) + \sum_{j \neq i} \eta_{ij}(p_i - p_j) = 0, \quad \Omega \times (0, T), \quad (5)$$

where $i = 1, \dots, M$ and M is the number of continua.

For the mechanics of the poroelastic multicontinuum media, we use an effective equation for displacement and have following poroelasticity problem for multicontinuum media

$$\begin{aligned} c_i \frac{\partial^{\alpha_i} p_i}{\partial t^{\alpha_i}} + \gamma_i \frac{\partial^{\beta_i} \text{div } \mathbf{u}}{\partial t^{\beta_i}} - \nabla \cdot (k_i \nabla p_i) + \sum_{j \neq i} \eta_{ij}(p_i - p_j) &= 0, \quad \Omega \times (0, T), \quad i = 1, \dots, M, \\ -\nabla \cdot \boldsymbol{\sigma}(\mathbf{u}) + \sum_j \gamma_j \nabla p_j &= 0, \quad \Omega \times (0, T), \end{aligned} \quad (6)$$

where $\boldsymbol{\sigma}$ denotes the stress tensor, \mathbf{u} the displacement, γ_i the Biot coefficient, M_i the Biot modulus ($c_i = \frac{1}{M_i}$) for the i -th component. In the case of a linear elastic stress-strain constitutive relation, we have

$$\boldsymbol{\sigma}(\mathbf{u}) = 2\mu \boldsymbol{\varepsilon}(\mathbf{u}) + \lambda \text{div } \mathbf{u} \mathcal{I}, \quad \boldsymbol{\varepsilon}(\mathbf{u}) = \frac{1}{2}(\nabla \mathbf{u} + \nabla \mathbf{u}^T),$$

where $\boldsymbol{\varepsilon}$ is the strain tensor, λ and μ are the Lamé's coefficients. Here we have a volume force sources that proportional to the sum of the pressure gradients for each continuum.

In the presented poroelasticity model (6), the fractional time parameters α_i and β_i are used to simulate the effects of history on porous media flow, where α_i is used for the effects of flow (pressure) history and β_i for the effects of mechanics (displacements) history on flow processes in multicontinuum media.

Next, we will concentrate on the triple continuum poroelasticity model:

$$\begin{aligned}
c_1 \frac{\partial^{\alpha_1} p_1}{\partial t^{\alpha_1}} + \gamma_1 \frac{\partial^{\beta_1} \operatorname{div} \mathbf{u}}{\partial t^{\beta_1}} - \nabla \cdot (k_1 \nabla p_1) + \eta_{12}(p_1 - p_2) + \eta_{1f}(p_1 - p_f) &= 0, \quad \Omega \times (0, T), \\
c_2 \frac{\partial^{\alpha_2} p_2}{\partial t^{\alpha_2}} + \gamma_2 \frac{\partial^{\beta_2} \operatorname{div} \mathbf{u}}{\partial t^{\beta_2}} - \nabla \cdot (k_2 \nabla p_2) + \eta_{12}(p_2 - p_1) + \eta_{2f}(p_2 - p_f) &= 0, \quad \Omega \times (0, T), \\
c_f \frac{\partial^{\alpha_f} p_f}{\partial t^{\alpha_f}} + \gamma_f \frac{\partial^{\beta_f} \operatorname{div} \mathbf{u}}{\partial t^{\beta_f}} - \nabla \cdot (k_f \nabla p_f) + \eta_{1f}(p_f - p_1) + \eta_{2f}(p_f - p_2) &= 0, \quad \gamma \times (0, T), \\
-\operatorname{div} \boldsymbol{\sigma}(\mathbf{u}) + \gamma_1 \nabla p_1 + \gamma_2 \nabla p_2 + \gamma_f \nabla p_f &= 0, \quad \Omega \times (0, T),
\end{aligned} \tag{7}$$

where the first continuum describes a flow in the matrix of the porous media, the second continuum belongs to the network of small highly connected fracture network (natural fractures) and the third continuum relates to the flow in low dimensional fracture networks.

3 Fine grid approximation using FEM

For the temporal approximation, we use an uniform mesh with N_T time steps and time step size $\tau = \frac{T}{N_T}$, where T is the final time for simulation. The values of a pressures and displacement at the time $t^n = n\tau$ ($n = 0, 1, 2, \dots, N_T$) are denoted by $(p_i^n, \mathbf{u}^n) = (p_i(t^n), \mathbf{u}(t^n))$, where p_i is the pressure of the i -th continuum.

The fractional-order derivative of the function v^n is defined using the following formula: add references here

$$\frac{\partial^{\alpha} v^n}{\partial t^{\alpha}} \approx \zeta_{\tau}^{(\alpha)} \left(v^n - v^{n-1} + \sum_{j=2}^n \zeta_{j-1}^{(\alpha)} (v^{n-j+1} - v^{n-j}) \right),$$

where

$$\zeta_{\tau}^{(\alpha)} = \frac{1}{\tau^{\alpha} \Gamma(2 - \alpha)}, \quad \zeta_{j-1}^{(\alpha)} = j^{1-\alpha} - (j-1)^{1-\alpha}.$$

For the spatial approximation, we use the finite element method. Let $V = [H^1(\Omega)]^d$, $W_1 = W_2 = H^1(\Omega)$ and $W_f = H^1(\gamma)$. The variational formulation of the poroelasticity problem in multicontinuum media (7) can be written as follows: given $(p_1^0, p_2^0, p_f^0, \mathbf{u}^0) \in W_1 \times W_2 \times W_f \times V$ iteratively find $(p_1^n, p_2^n, p_f^n, \mathbf{u}^n) \in W_1 \times W_2 \times W_f \times V$ such that

$$\begin{aligned}
&\zeta_{\tau}^{(\alpha_i)} m_i(p_i^n - p_i^{n-1}, w_i) + \zeta_{\tau}^{(\alpha_i)} \sum_{j=2}^n \zeta_{j-1}^{(\alpha_i)} m_i(p_i^{n-j+1} - p_i^{n-j}, w_i) \\
&\quad + \zeta_{\tau}^{(\beta_i)} d_i(\mathbf{u}^n - \mathbf{u}^{n-1}, w_i) + \zeta_{\tau}^{(\beta_i)} \sum_{j=2}^n \zeta_{j-1}^{(\beta_i)} d_i(\mathbf{u}^{n-j+1} - \mathbf{u}^{n-j}, w_i) \\
&\quad + b_i(p_i^n, w_i) + \sum_{j \neq i} q_{ij}(p_i^n - p_j^n, w_i) = 0, \quad \forall w_i \in W_i, i = 1, 2, f, \\
&\quad a(\mathbf{u}^n, \mathbf{v}) + \sum_j g_j(p_j^n, \mathbf{v}) = 0, \quad \forall \mathbf{v} \in V,
\end{aligned} \tag{8}$$

where

$$\begin{aligned}
b_i(p_i, w_i) &= \int_{\Omega_i} k_i \nabla p_i \cdot \nabla w_i dx, \quad a(\mathbf{u}, \mathbf{v}) = \int_{\Omega} \boldsymbol{\sigma}(\mathbf{u}) \cdot \boldsymbol{\varepsilon}(\mathbf{v}) dx, \\
m_i(p_i, w_i) &= \int_{\Omega_i} c_i p_i w_i dx, \quad q_{ij}(p_i - p_j, w_i) = \int_{\Omega_i} \eta_{ij}(p_i - p_j) w_i dx,
\end{aligned}$$

$$d_i(\mathbf{u}, w_i) = \int_{\Omega_i} \gamma_i \operatorname{div} \mathbf{u} w_i dx, \quad g_i(p_i, \mathbf{v}) = \int_{\Omega_i} \gamma_i \nabla p_i \mathbf{v} dx,$$

for $i, j = 1, 2, f$, with $\Omega_1 = \Omega_2 = \Omega$, $\Omega_f = \gamma$.

Let \mathcal{T}^h denote a finite element partition of the domain Ω and \mathcal{E}_h is the set of all the interfaces between the elements \mathcal{T}_h . For the fracture continuum, we use a discrete fracture model and use an unstructured fine grid \mathcal{T}^h that explicitly resolve fracture geometry. We assume that $\mathcal{E}_\gamma = \cup_j \gamma_j$ is the subset of faces for \mathcal{T}^h that represent fractures, where $j = 1, \dots, N_{frac}$, N_{frac} is the number of discrete fractures and $\mathcal{E}_\gamma \subset \mathcal{E}_h$ be the subset of all faces that represent fractures. Moreover, \mathcal{E}_γ describe the lower dimensional fracture grid.

For $i = 1, 2, f$, let

$$p_i = \sum_l p_{i,l}^h \phi_l^i, \quad \mathbf{u} = \sum_l u_l^h \Phi_l,$$

where $\{\Phi_l\}$ is the basis for displacements, $\{\phi_l^i\}$, $i = 1, 2$, the d -dimensional bases for pressure, and $\{\phi_l^f\}$ the $(d-1)$ -dimensional basis for pressure. Then we have following discrete system in matrix form on the fine grid for the triple-continuum media

$$\begin{aligned} & \zeta_\tau^{(\alpha_i)} M_i p_i^n + \zeta_\tau^{(\beta_i)} D_i \mathbf{u}^n + A_i p_i^n + \sum_{j \neq i} Q_{ij} (p_i^n - p_j^n) \\ &= \zeta_\tau^{(\alpha_i)} M_i p_i^{n-1} - \zeta_\tau^{(\alpha_i)} \sum_{j=2}^n \zeta_{j-1}^{(\alpha_i)} M_i (p_i^{n-j+1} - p_i^{n-j}) \\ &+ \zeta_\tau^{(\beta_i)} D_i \mathbf{u}^{n-1} - \zeta_\tau^{(\beta_i)} \sum_{j=2}^n \zeta_{j-1}^{(\beta_i)} D_i (\mathbf{u}^{n-j+1} - \mathbf{u}^{n-j}), \quad \text{for } i = 1, 2, f, \\ & \sum_j D_j^T p_j^n + A_u \mathbf{u}^n = 0, \end{aligned} \tag{9}$$

where the indices i and n stand for the continuum and the time step, respectively, and

$$\begin{aligned} A_i &= [a_{i,ln}], \quad a_{i,ln} = \int_{\Omega_i} k_i \nabla \phi_l^i \cdot \nabla \phi_n^i dx, \quad A_u = [a_{u,ln}], \quad a_{u,ln} = \int_{\Omega} \boldsymbol{\sigma}(\Phi_l) \cdot \boldsymbol{\varepsilon}(\Phi_n) dx, \\ M_i &= [c_{i,ln}], \quad m_{i,ln} = \int_{\Omega_i} c_i \phi_l^i \phi_n^i dx, \quad Q_{ij} = [q_{ij,ln}], \quad q_{ij,ln} = \int_{\Omega_i} \eta_{ij} \phi_l^i \phi_n^j dx, \\ D_i &= [d_{i,ln}], \quad d_{i,ln} = \int_{\Omega} \gamma_i \operatorname{div} \Phi_l \phi_n^i dx. \end{aligned}$$

4 Coarse grid approximation using GMsFEM

For the coarse grid approximation, we use the Generalized Multiscale Finite Element Method (GMsFEM). We construct multiscale basis functions for displacements and pressures separately, but basis functions for multicontinuum pressure equations are constructed in a coupled way.

Denote by \mathcal{T}^H the coarse grid partitioning of the domain

$$\mathcal{T}^H = \bigcup_j K_j,$$

where K_j 's are coarse grid cells. We will use the standard continuous P_1 Galerkin approximation on the coarse grid, and define local domain ω_l for multiscale basis functions as combination of the several coarse grid cells that share same coarse grid nodes ($l = 1, \dots, N_v^H$, N_v^H being the number of coarse grid vertices).

4.1 Multiscale basis functions for pressures in multicontinuum media

To construct a snapshot space, we solve the following local problem in domain ω_l : find $\psi^{l,j} = (\psi_1^{l,j}, \psi_2^{l,j}, \psi_f^{l,j}) \in W_1^h \times W_2^h \times W_f^h$ such that

$$b_i(\psi_i^{l,j}, w_i) + \sum_j q_{ij}(\psi_i^{l,j} - \psi_j^{l,j}, w_i) = 0, \quad \forall w_i \in \hat{W}_i^h, \quad i = 1, 2, f, \quad (10)$$

where

$$W_i^h = \{w \in H^1(\omega_l) : w = \delta_i^j \text{ on } \partial\omega_l\}, \quad \hat{W}_i^h = \{w \in H^1(\omega_l) : w = 0 \text{ on } \partial\omega_l\},$$

and δ_i^j is the piecewise constant function (delta function) for $j = 1, \dots, N_v^{\omega_l}$ ($N_v^{\omega_l}$ is the number of nodes on the computation mesh for ω_l), i is the index of continuum ($i = 1, 2, f$). Therefore, we solve $L_p^{\omega_l} = 3N_v^{\omega_l}$ local problems.

We define a snapshot space for pressures in multicontinuum media as follows.

$$W_{snap}(\omega_l) = \text{span}\{\psi^{l,j}, l = 1, \dots, N_v^H, j = 1, \dots, L_p^{\omega_l}\}. \quad (11)$$

Next, we solve the following local spectral problem on the snapshot space:

$$\tilde{A}_p \tilde{\phi}^l = \lambda_p \tilde{S}_p \tilde{\phi}^l, \quad (12)$$

where $\tilde{\phi}^l = (R_{snap}^p)^T \phi^l$ and

$$\tilde{A}_p = R_{snap}^p A_p (R_{snap}^p)^T, \quad \tilde{S}_p = R_{snap}^p S_p (R_{snap}^p)^T, \quad R_{snap}^p = (\psi^{l,1}, \dots, \psi^{l,L_p^{\omega_l}})^T$$

Here for matrices in triple continuum case, we have

$$S_p = \begin{pmatrix} S_1 & 0 & 0 \\ 0 & S_2 & 0 \\ 0 & 0 & S_f \end{pmatrix}, \quad A_p = \begin{pmatrix} A_1 + Q_{12} + Q_{1f} & -Q_{12} & -Q_{1f} \\ -Q_{12} & A_2 + Q_{12} + Q_{2f} & -Q_{2f} \\ -Q_{1f} & -Q_{2f} & A_f + Q_{1f} + Q_{2f} \end{pmatrix}$$

where

$$A_i = [a_{i,mn}], \quad a_{i,mn} = \int_{\omega_i^i} k_i \text{grad } \phi_m^i \cdot \text{grad } \phi_n^i dx, \quad S_i = [s_{i,mn}], \quad s_{i,mn} = \int_{\omega_i^i} k_i \phi_m^i \phi_n^i dx.$$

We choose an eigenvector $\hat{\phi}_j$ ($j = 1, \dots, M^{l,p}$) corresponding to the first smallest $M^{l,p}$ eigenvalues and multiply to the linear partition of unity functions χ^l for obtaining conforming basis functions

$$W_{ms} = \text{span}\{\phi^{l,j}, l = 1, \dots, N_v^H, j = 1, \dots, M^{l,p}\},$$

where $\phi^{l,j} = \chi^l \hat{\phi}^{l,j}$.

4.2 Multiscale basis functions for displacements

We construct the multiscale basis functions by solution following problem in local domain ω_l : find $\Psi^{l,j} \in V^h$ such that

$$a(\Psi^{l,j}, \mathbf{v}) = 0, \quad \forall \mathbf{v} \in \hat{V}^h, \quad (13)$$

where

$$V^h = \{\mathbf{v} \in H^1(\omega_l) : \mathbf{v} = \bar{\delta}_i^j \text{ on } \partial\omega_l\}, \quad \hat{V}^h = \{\mathbf{v} \in H^1(\omega_l) : \mathbf{v} = 0 \text{ on } \partial\omega_l\}.$$

and $\bar{\delta}_i^j$ is the vector for each component for d -dimensional problem ($d = 2, 3$) i.e. $\bar{\delta}_i^j = (\delta_i^j, 0, 0)$ or $\bar{\delta}_i^j = (0, \delta_i^j, 0)$ or $\bar{\delta}_i^j = (0, 0, \delta_i^j)$ for $d = 3$. We solve $L_u^{\omega_l} = d \cdot N_v^{\omega_l}$ local problems.

We define snapshot space for pressures in multicontinuum media as follows

$$V_{snap}(\omega_l) = \text{span}\{\Psi^{l,j}, l = 1, \dots, N_v^H, j = 1, \dots, L_u^{\omega_l}\}. \quad (14)$$

For the construction of multiscale basis, we solve the following local spectral problem on the snapshot space:

$$\tilde{A}_u \tilde{\Phi} = \lambda_u \tilde{S}_u \tilde{\Phi}, \quad (15)$$

where $\hat{\Phi}^l = (R_{snap}^u)^T \tilde{\Phi}^l$,

$$\tilde{A}_u = R_{snap}^u A_u (R_{snap}^u)^T, \quad \tilde{S}_u = R_{snap}^u S_u (R_{snap}^u)^T, \quad R_{snap}^u = (\Psi^{l,1}, \dots, \Psi^{l,L_u^{\omega_l}})^T$$

and

$$A_u = [a_{u,mn}], \quad a_{u,mn} = \int_{\omega_l} \boldsymbol{\sigma}(\Phi_m) \cdot \boldsymbol{\varepsilon}(\Phi_n) dx, \quad S_u = [s_{i,mn}], \quad s_{i,mn} = \int_{\omega_l} (\lambda + 2\mu) \Phi_m^i \Phi_n^i dx.$$

We choose eigenvectors $\hat{\Phi}_j, j = 1, \dots, M^{l,u}$ corresponding to the first smallest $M^{l,u}$ eigenvalues and multiply by the linear partition of unity functions to obtain the conforming basis functions:

$$V_{ms} = \text{span}\{\Phi^{l,j}, l = 1, \dots, N_v^H, j = 1, \dots, M^{l,u}\},$$

where $\Phi^{l,j} = \chi^l \hat{\Phi}^{l,j}$.

4.3 Coarse grid system

. Using the above constructed multiscale basis functions for pressures and displacements, we define the projection matrix:

$$R = \begin{pmatrix} R_p & 0 \\ 0 & R_u \end{pmatrix}, \quad (16)$$

where

$$R_u = (\Phi^{1,1}, \dots, \Phi^{1,M^{1,u}}, \dots, \Phi^{N_v^H,1}, \dots, \Phi^{N_v^H,M^{N_v^H,u}})^T, \\ R_p = (\phi^{1,1}, \dots, \phi^{1,M^{1,p}}, \dots, \phi^{N_v^H,1}, \dots, \phi^{N_v^H,M^{N_v^H,p}})^T.$$

Then we obtain the following reduced order model:

$$\begin{aligned} & \zeta_\tau^{(\alpha_i)} M_i^H p_i^{H,n} + \zeta_\tau^{(\beta_i)} D_i^H \mathbf{u}^{H,n} + A_i^H p_i^{H,n} + \sum_{j^!=i} Q_{ij}^H (p_i^{H,n} - p_j^{H,n}) \\ &= \zeta_\tau^{(\alpha_i)} M_i^H p_i^{H,n-1} - \zeta_\tau^{(\alpha_i)} \sum_{j=2}^n \zeta_{j-1}^{(\alpha_i)} M_i^H (p_i^{H,n-j+1} - p_i^{H,n-j}) \\ &+ \zeta_\tau^{(\beta_i)} D_i^H \mathbf{u}^{H,n-1} - \zeta_\tau^{(\beta_i)} \sum_{j=2}^n \zeta_{j-1}^{(\beta_i)} D_i^H (\mathbf{u}^{H,n-j+1} - \mathbf{u}^{H,n-j}), \\ & \sum_j (D_j^H)^T p_j^{H,n} + A_u^H \mathbf{u}^{H,n} = 0, \end{aligned} \quad (17)$$

where

$$M_i^H = R M_i R^T, \quad A_i^H = R A_i R^T, \quad Q_{ij}^H = R Q_{ij} R^T, \quad D_i^H = R D_i R^T, \quad A_u^H = R A_u R^T.$$

After obtaining the coarse-scale solutions, we reconstruct the fine-scale solutions:

$$p_i^{ms,n} = R^T p_i^{H,n}, \quad u^{ms,n} = R^T u^{H,n}.$$

We remark that in our method presented above we store and use only the information on the coarse-grid solutions at the previous time step.

5 Numerical results

In this section, we present the numerical results of the poroelasticity problems in heterogeneous and fractured media with fractional derivatives. The coarse grid is uniform with rectangular cells. In Figure 1, we show computational coarse and fine grids. The fine grid contains 25846 cells and 12944 vertices, and the coarse grid contains 121 vertices and 100 cells. We consider the time-fractional diffusion equation for poroelasticity problem in $\Omega = (0, 50)^2$ for two cases such as the poroelasticity in fractured media and multicontinuum media. For coefficients representing matrix and fracture properties, we set $\gamma_1 = 0.1, \gamma_2 = 0.1, \gamma_f = 0, k_f = 1.0, M_1 = M_2 = 10, M_f = 10^3, \nu = 0.3$. The calculation is performed by $T_{max} = 86400$ with times step $\tau = 8640$ and $\eta_{12} = 5 * k_2$. Heterogeneous coefficients for elasticity modulus and heterogeneous permeability for the first and second continua are presented in Fig. 2. A numerical solution is presented with the following boundary conditions $u_x = 0, \sigma_y = 0, x \in \Gamma_L \cup \Gamma_R, u_y = 0, \sigma_x = 0, x \in \Gamma_T \cup \Gamma_B$ for displacement, and the initial condition $p^0 = 1$ for pressure.

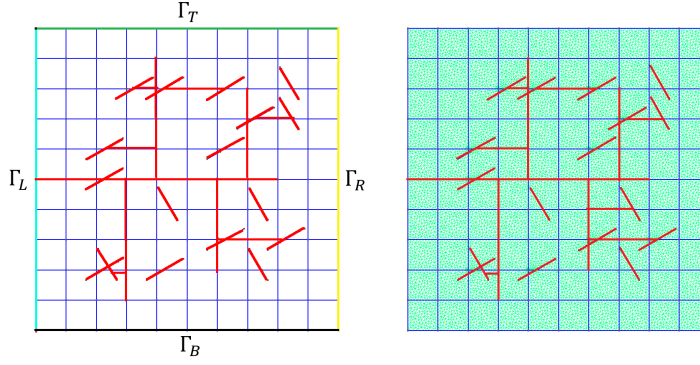


Figure 1: Computation domain and grids. Coarse grid (blue color), fine grid (green), and fractures (red).

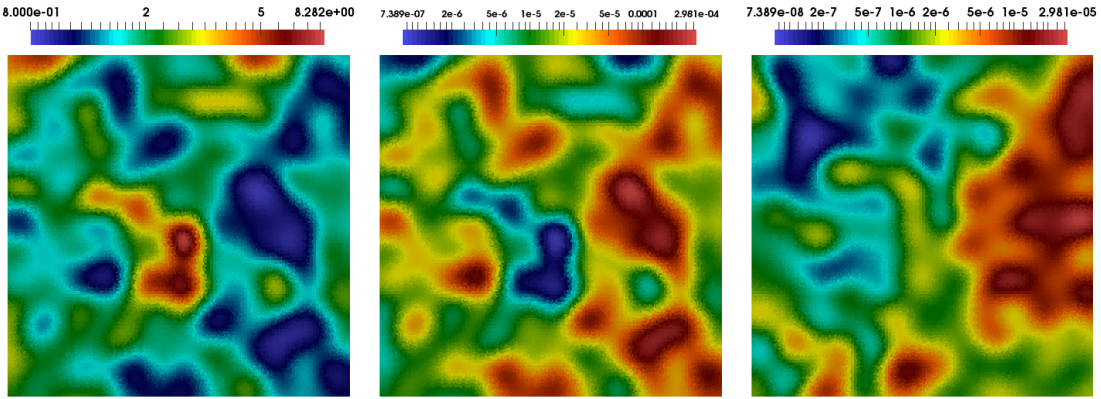


Figure 2: Elasticity coefficient E (left) and heterogeneous permeability k_1 (center) and k_2 (right).

To compare the results, we use the fine grid solution as a reference solution and calculate relative L_2 norm and H_1 semi-norm of errors between the multiscale and reference solutions

$$e_{L^2}^{p_i} = \left(\frac{(p_i - p_i^{ms}, p_i - p_i^{ms})}{(p_i, p_i)} \right)^{1/2}, \quad e_{L^2}^u = \left(\frac{(\mathbf{u} - \mathbf{u}^{ms}, \mathbf{u} - \mathbf{u}^{ms})}{(\mathbf{u}, \mathbf{u})} \right)^{1/2},$$

$$e_{H_1}^{p_i} = \left(\frac{b(p_i - p_i^{ms}, p_i - p_i^{ms})}{b(p_i, p_i)} \right)^{1/2}, \quad e_{H_1}^u = \left(\frac{a(\mathbf{u} - \mathbf{u}^{ms}, \mathbf{u} - \mathbf{u}^{ms})}{a(\mathbf{u}, \mathbf{u})} \right)^{1/2},$$

where i is the index for the continuum ($i = 1, 2$), and $y^{ms} = (p_1^{ms}, p_2^{ms}, \mathbf{u}^{ms})$ denotes the multiscale solution using the GMsFEM and $y = (p_1, p_2, \mathbf{u})$ the fine grid solution.

5.1 Poroelasticity in fractured media

We present how the introduction of the time memory effect, by means of the Caputo's fractional time derivative in the constitutive equation, affects both the pressure and displacement in fractured media. In this subsection, we solve the poroelasticity problem with one continuum.

In Figure 3 we present the numerical solution distribution of pressure at different time steps on a fine mesh with other fractional order derivative. Relative L_2 and energy H_1 errors are presented for different number of multiscale basis functions in Tables 1 – 3. We present the error comparison between the fine-scale and multiscale solutions with different numbers of multiscale basis functions. We observe that the error decreases when we increase the number of multiscale basis functions for each fractional order derivative. The relative error reduces from 21% to 0.8% for displacement and 12% to 0.4% for pressure with fractional order derivative $\alpha = 1.0$. To obtain a good solution, we need to take twelve basis functions in each fractional order derivative.

Next, the relative L_2 error dynamics in % for different number of multiscale basis functions with fractional order derivative $\alpha = 1.0$ are shown in Figure 4. We observe that the errors reduce by time. In Figure 5 we present relative L_2 error dynamics with different fractional order derivative for twelve multiscale basis functions. The behavior of the figures is similar to the previous figures. Therefore, we can assume that the method provides a good solution.

Figures 6 – 8 show the distribution of pressure and displacement along X and Y directions at final time for different fractional order derivatives. In the first row, we show fine scale and multiscale solutions with twelve multiscale basis functions for the GMsFEM is presented in the second row. We observe good results of the presented method for solving poroelasticity problems for different fractional order derivatives.

| M | DOF_H | $e_{L_2}^u$ (%) | $e_{H_1}^u$ (%) | $e_{L_2}^p$ (%) | $e_{H_1}^p$ (%) |
|-----|---------|-----------------|-----------------|-----------------|-----------------|
| 1 | 363 | 26.324 | 62.768 | 18.280 | 80.061 |
| 2 | 726 | 14.436 | 40.353 | 13.540 | 64.607 |
| 4 | 1452 | 7.355 | 30.629 | 6.734 | 40.175 |
| 8 | 2904 | 3.641 | 21.532 | 3.149 | 25.884 |
| 12 | 4356 | 2.580 | 18.158 | 2.261 | 20.837 |
| 16 | 5808 | 2.112 | 16.312 | 1.896 | 18.730 |

Table 1: Relative errors for displacement and pressure with different numbers of multiscale basis functions. Poroelasticity in fractured media with fractional order derivative $\alpha = 0.8$

| M | DOF_H | $e_{L_2}^u$ (%) | $e_{H_1}^u$ (%) | $e_{L_2}^p$ (%) | $e_{H_1}^p$ (%) |
|-----|---------|-----------------|-----------------|-----------------|-----------------|
| 1 | 363 | 21.975 | 48.612 | 14.909 | 69.075 |
| 2 | 726 | 10.425 | 28.102 | 9.898 | 54.202 |
| 4 | 1452 | 4.112 | 20.956 | 3.651 | 29.799 |
| 8 | 2904 | 1.803 | 10.888 | 1.406 | 17.002 |
| 12 | 4356 | 1.333 | 8.603 | 1.027 | 14.209 |
| 16 | 5808 | 1.115 | 7.463 | 0.872 | 13.023 |

Table 2: Relative errors for displacement and pressure with different numbers of multiscale basis functions. Poroelasticity in fractured media with fractional order derivative $\alpha = 0.9$

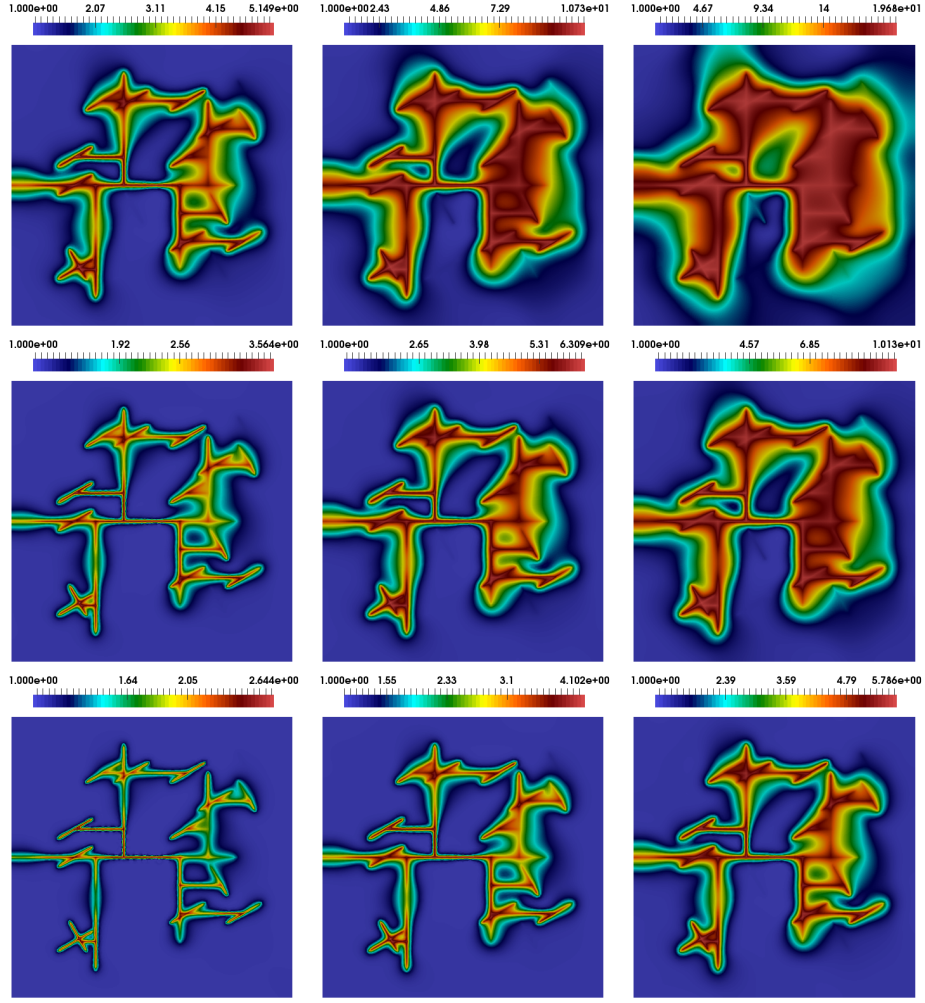


Figure 3: Distribution of pressure for exact solution for $t = 0, 25920$ and $t = 86400$ (from left to right). First row: fractional order derivative $\alpha = 1.0$. Second row: fractional order derivative $\alpha = 0.9$. Third row: fractional order derivative $\alpha = 0.8$.

| M | DOF_H | $e_{L_2}^u$ (%) | $e_{H_1}^u$ (%) | $e_{L_2}^p$ (%) | $e_{H_1}^p$ (%) |
|-----|---------|-----------------|-----------------|-----------------|-----------------|
| 1 | 363 | 21.461 | 40.372 | 12.348 | 61.024 |
| 2 | 726 | 9.611 | 21.865 | 6.983 | 45.957 |
| 4 | 1452 | 2.959 | 14.532 | 1.979 | 22.994 |
| 8 | 2904 | 1.341 | 7.890 | 0.680 | 12.675 |
| 12 | 4356 | 1.017 | 6.256 | 0.510 | 10.780 |
| 16 | 5808 | 0.871 | 5.402 | 0.450 | 10.063 |

Table 3: Relative errors for displacement and pressure with different numbers of multiscale basis functions. Poroelasticity in fractured media with fractional order derivative $\alpha = 1.0$

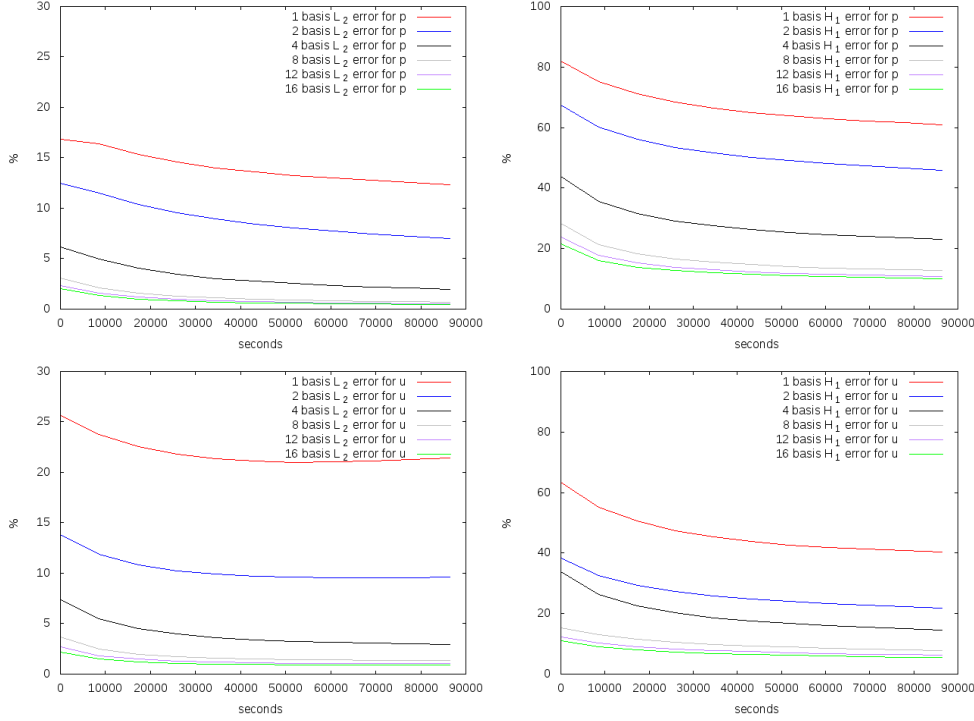


Figure 4: Poroelasticity in fractured media: Relative L_2 error (left) and H_1 (right) errors vs time for different number multiscale basis functions for pressure (first row) and displacements (second row) with fractional order derivative $\alpha = 1.0$.

5.2 Poroelasticity in multicontinuum media

Next we consider a computational macroscopic model for fractional Biot's system in multicontinuum heterogeneous media. In this case, we consider two continua. In this part of the work, we investigate a time memory formalism in poroelasticity problem in multicontinuum media.

In Tables 4-6 relative L_2 and H_1 -energy errors are presented for different number of multiscale basis functions. The results show that twelve multiscale basis functions are enough to achieve good results, for example, for fractional order derivative $\alpha = 1.0$ with 1.051% of L_2 error for displacement, 0.667% and 0.644% of L_2 errors for the first and second continuum pressures. We have similar improvements for further increment of the multiscale basis functions.

Then the relative L_2 error dynamics in % for different number of multiscale basis functions with fractional order derivative $\alpha = 1.0$ are shown in Figure 9. We also observe that errors reduce by time for poroelasticity in multicontinuum media. In Figure 10 we present relative L_2 error dynamics with different fractional order derivative for twelve multiscale basis functions. We observe that the presented method provides good results for different fractional order derivatives.

The distribution of pressure for the first and second continua, displacement along x and y directions at final time are presented in Figures 11 – 13. In the first row, we depict a reference fine grid solution and multiscale solution with twelve multiscale basis functions for the GmsFEM is presented in second row. We observe good accuracy comparing the fine-scale solution with the multiscale solution with twelve basis functions for displacement along x and y direction and pressures for different fractional order derivatives. For the poroelasticity problems in multicontinuum media, we also observe good convergences.

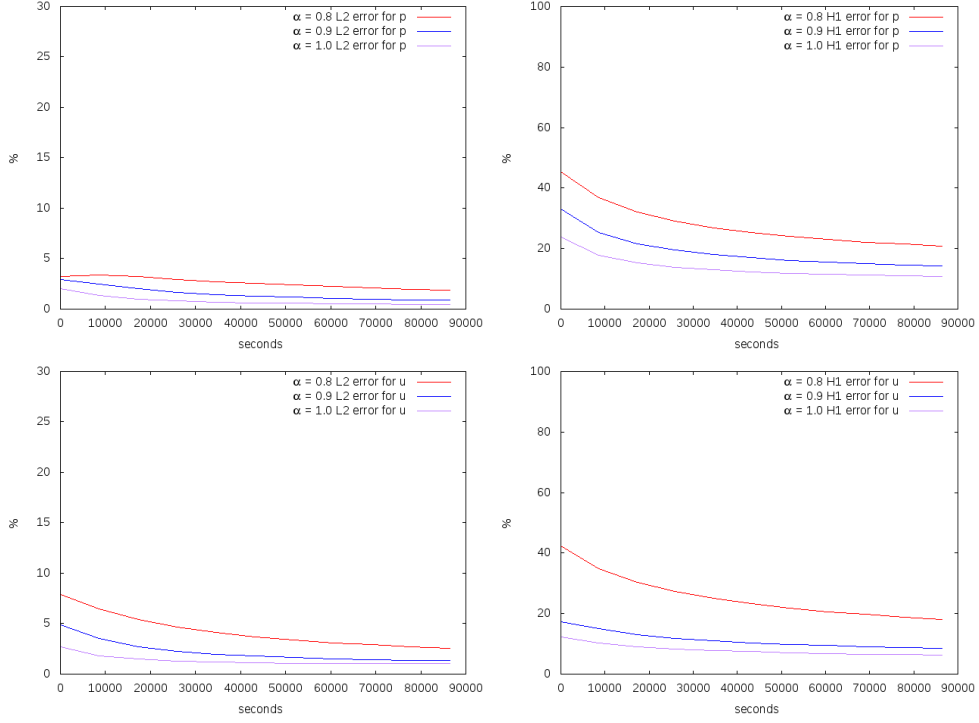


Figure 5: Poroelasticity in fractured media: Relative L_2 error (left) and H_1 (right) errors vs time for different fractional order derivative($\alpha = 0.8, 0.9, 1.0$) for pressure (first row) and displacements (second row) with multiscale basis function 12.

| M | DOF_H | $e_{L_2}^u$ (%) | $e_{H_1}^u$ (%) | $e_{L_2}^{p_1}$ (%) | $e_{H_1}^{p_1}$ (%) | $e_{L_2}^{p_2}$ (%) | $e_{H_1}^{p_2}$ (%) |
|-----|---------|-----------------|-----------------|---------------------|---------------------|---------------------|---------------------|
| 1 | 484 | 26.201 | 64.703 | 17.893 | 83.608 | 13.191 | 78.062 |
| 2 | 968 | 14.965 | 43.514 | 13.705 | 68.893 | 9.745 | 65.278 |
| 4 | 1936 | 8.201 | 33.273 | 6.753 | 43.739 | 4.696 | 39.658 |
| 8 | 3872 | 4.142 | 23.807 | 3.350 | 27.219 | 2.315 | 26.418 |
| 12 | 5808 | 2.984 | 20.126 | 2.528 | 22.687 | 1.779 | 22.887 |
| 16 | 7744 | 2.440 | 18.097 | 2.154 | 20.365 | 1.528 | 21.085 |

Table 4: Relative errors for displacement and pressure with different numbers of multiscale basis functions. Poroelasticity in multicontinuum media with fractional order derivative $\alpha = 0.8$

| M | DOF_H | $e_{L_2}^u$ (%) | $e_{H_1}^u$ (%) | $e_{L_2}^{p_1}$ (%) | $e_{H_1}^{p_1}$ (%) | $e_{L_2}^{p_2}$ (%) | $e_{H_1}^{p_2}$ (%) |
|-----|---------|-----------------|-----------------|---------------------|---------------------|---------------------|---------------------|
| 1 | 484 | 22.431 | 53.276 | 15.457 | 73.825 | 14.153 | 66.143 |
| 2 | 968 | 11.122 | 31.456 | 10.879 | 58.526 | 9.623 | 53.550 |
| 4 | 1936 | 4.931 | 21.444 | 4.369 | 33.371 | 3.885 | 30.638 |
| 8 | 3872 | 2.264 | 14.665 | 1.866 | 19.661 | 1.678 | 18.949 |
| 12 | 5808 | 1.629 | 12.265 | 1.355 | 16.404 | 1.234 | 16.020 |
| 16 | 7744 | 1.335 | 10.942 | 1.167 | 14.948 | 1.061 | 14.730 |

Table 5: Relative errors for displacement and pressure with different numbers of multiscale basis functions. Poroelasticity in multicontinuum media with fractional order derivative $\alpha = 0.9$

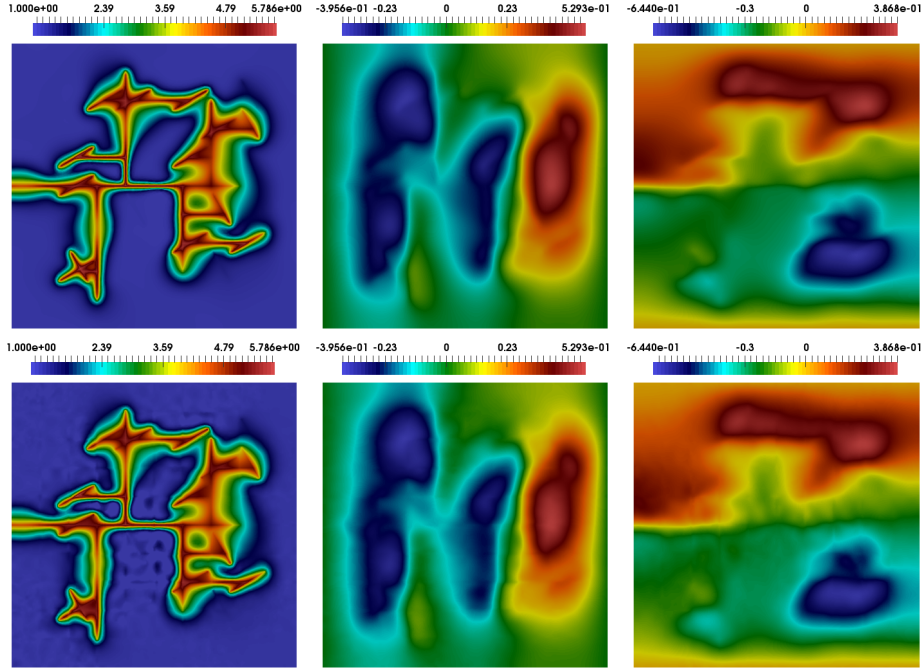


Figure 6: Poroelasticity in fractured media: Distribution of pressure and displacement along X and Y (from left to right) at final time for fractional order derivative $\alpha = 0.8$. First row: exact solution. Second row: multiscale solution(12 multiscale basis functions).

| M | DOF_H | $e_{L_2}^u$ (%) | $e_{H_1}^u$ (%) | $e_{L_2}^{p_1}$ (%) | $e_{H_1}^{p_1}$ (%) | $e_{L_2}^{p_2}$ (%) | $e_{H_1}^{p_2}$ (%) |
|-----|---------|-----------------|-----------------|---------------------|---------------------|---------------------|---------------------|
| 1 | 484 | 20.226 | 44.876 | 12.573 | 63.923 | 12.272 | 56.038 |
| 2 | 968 | 8.981 | 23.888 | 7.720 | 48.952 | 7.391 | 43.954 |
| 4 | 1936 | 3.255 | 14.252 | 2.404 | 25.288 | 2.290 | 23.452 |
| 8 | 3872 | 1.440 | 9.519 | 0.922 | 14.563 | 0.904 | 13.362 |
| 12 | 5808 | 1.051 | 7.925 | 0.667 | 12.349 | 0.644 | 11.017 |
| 16 | 7744 | 0.876 | 7.059 | 0.579 | 11.422 | 0.553 | 10.100 |

Table 6: Relative errors for displacement and pressure with different numbers of multiscale basis functions. Poroelasticity in multicontinuum media with fractional order derivative $\alpha = 1.0$

6 Conclusion

In this paper, a mathematical formulation is introduced for poroelasticity problems in fractured and heterogeneous media with the time fractional derivatives. We assume the media have a multiscale nature and develop a computational macroscale model. A finite difference approximation of the Caputo fractional time derivative is adopted for flow and mechanics. Due to the time fractional order, the resulting system has a memory and requires storing the solutions at previous time steps. Because of multiple scales, we use the GMsFEM as a computational model. For the GMsFEM, one needs multiscale basis functions and a global formulation. We construct multiscale basis functions for the approximation of pressure and displacement and solve the problem on the coarse grid. The multiscale approach uses the Discrete Fracture Model to resolve the fractures on a fine grid. The numerical examples are presented to verify the efficiency of the proposed difference schemes for two-dimensional problem. We provide comparison results using different numbers of basis functions for the pressures in each continuum and the displacement

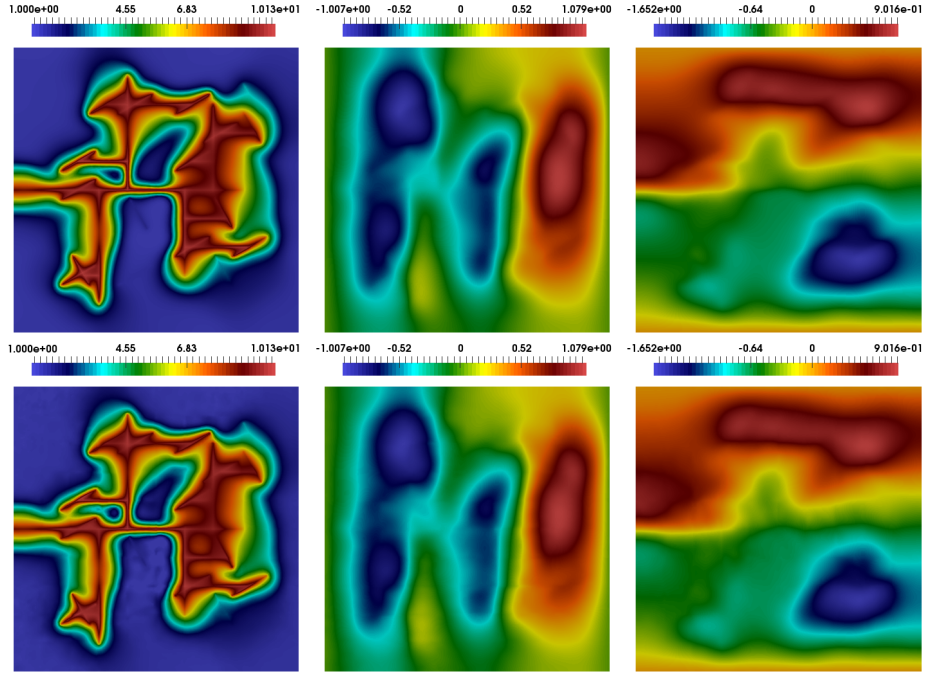


Figure 7: Poroelasticity in fractured media: Distribution of pressure and displacement along X and Y (from left to right) at final time for fractional order derivative $\alpha = 0.9$. First row: exact solution. Second row: multiscale solution(12 multiscale basis functions).

between the multiscale and fine-scale solutions with different fractional order derivative. Our results show that the proposed method can give accurate solutions.

Acknowledgments

The research of DS is supported in part by National Research Foundation (NRF-2017R1A2B3012506). The works of AA and AT are supported by North-Caucasus Center for Mathematical Research under agreement N. 075-02-2021-1749 with the Ministry of Science and Higher Education of the Russian Federation. AT is supported by Russian government project Science and Universities 121110900017-5 aimed at supporting junior laboratories. MV work is supported by the mega-grant of the Russian Federation Government №14.Y26.31.0013.

References

- [1] I. Y. Akkutlu, Y. Efendiev, and M. Vasilyeva. Multiscale model reduction for shale gas transport in fractured media. *Computational Geosciences*, pages 1–21, 2015.
- [2] I. Y. Akkutlu, Y. Efendiev, M. Vasilyeva, and Y. Wang. Multiscale model reduction for shale gas transport in a coupled discrete fracture and dual-continuum porous media. *Journal of Natural Gas Science and Engineering*, 48:65–76, 2017.
- [3] I. Y. Akkutlu, Y. Efendiev, M. Vasilyeva, and Y. Wang. Multiscale model reduction for shale gas transport in poroelastic fractured media. *Journal of Computational Physics*, 353:356–376, 2018.

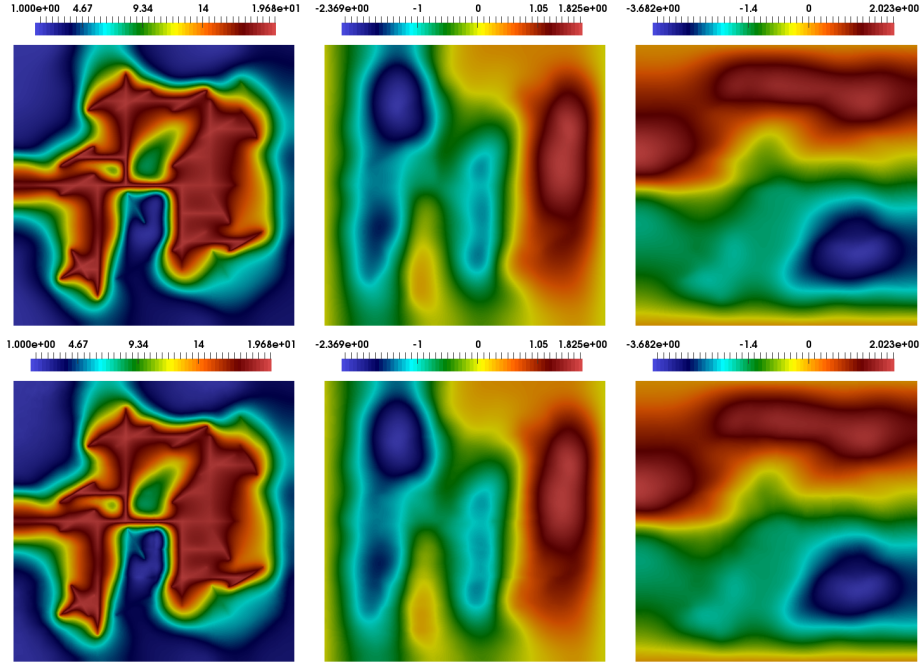


Figure 8: Poroelasticity in fractured media: Distribution of pressure and displacement along X and Y (from left to right) at final time for fractional order derivative $\alpha = 1.0$. First row: exact solution. Second row: multiscale solution(12 multiscale basis functions).

- [4] G. Alaimo, V. Piccolo, A. Cutolo, L. Deseri, M. Fraldi, and M. Zingales. A fractional order theory of poroelasticity. *Mechanics Research Communications*, 100:103395, 2019.
- [5] T. Arbogast, J. Douglas, Jr, and U. Hornung. Derivation of the double porosity model of single phase flow via homogenization theory. *SIAM Journal on Mathematical Analysis*, 21(4):823–836, 1990.
- [6] N. Bakhvalov and G. Panasenko. Homogenization in periodic media, mathematical problems of the mechanics of composite materials. ed: *Nauka, Moscow*, 1984.
- [7] M. A. Biot. General theory of three-dimensional consolidation. *Journal of applied physics*, 12(2):155–164, 1941.
- [8] M. A. Biot. Theory of elasticity and consolidation for a porous anisotropic solid. *Journal of applied physics*, 26(2):182–185, 1955.
- [9] D. L. Brown and M. Vasilyeva. A generalized multiscale finite element method for poroelasticity problems I: Linear problems. *Journal of Computational and Applied Mathematics*, 294:372–388, 2016.
- [10] D. L. Brown and M. Vasilyeva. A generalized multiscale finite element method for poroelasticity problems II: Nonlinear coupling. *Journal of Computational and Applied Mathematics*, 297:132–146, 2016.
- [11] M. Caputo. Vibrations of an infinite viscoelastic layer with a dissipative memory. *The Journal of the Acoustical Society of America*, 56(3):897–904, 1974.
- [12] M. Caputo and F. Mainardi. Linear models of dissipation in anelastic solids. *La Rivista del Nuovo Cimento (1971-1977)*, 1(2):161–198, 1971.

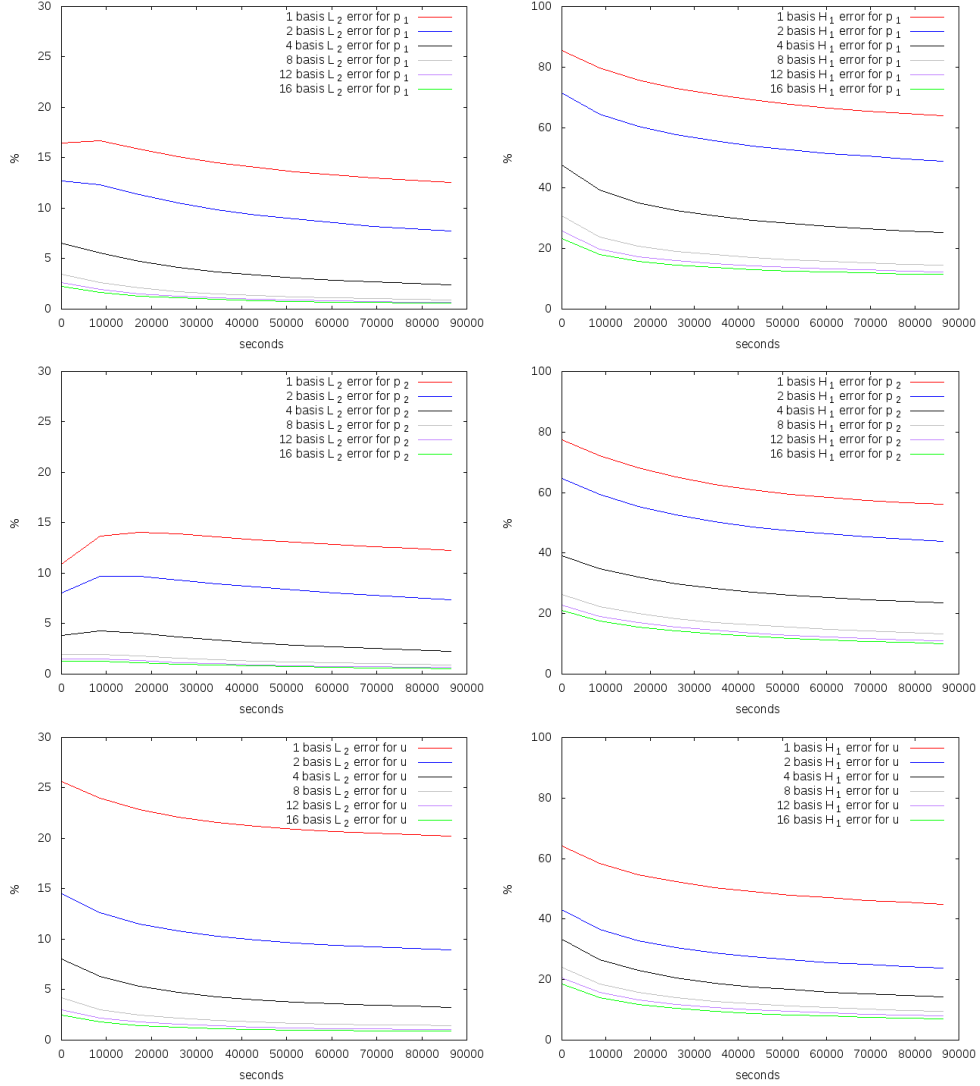


Figure 9: Poroelasticity in multicontinuum media: Relative L_2 error (left) and H_1 (right) errors vs time for different number multiscale basis functions for first continuum (first row), second continuum (second row) and displacements (third row) with fractional order derivative $\alpha = 1.0$.

- [13] J. M. Carcione, C. Morency, and J. E. Santos. Computational poroelasticity – Review. *Geophysics*, 75(5):75A229–75A243, 2010.
- [14] N. Castelletto, S. Klevtsov, H. Hajibeygi, and H. A. Tchelepi. Multiscale two-stage solver for Biot’s poroelasticity equations in subsurface media. *Computational Geosciences*, pages 1–18, 2018.
- [15] C. D’Angelo and A. Quarteroni. On the coupling of 1D and 3D diffusion-reaction equations: Application to tissue perfusion problems. *Mathematical Models and Methods in Applied Sciences*, 18(08):1481–1504, 2008.
- [16] C. D’Angelo and A. Scotti. A mixed finite element method for Darcy flow in fractured porous media with non-matching grids. *ESAIM: Mathematical Modelling and Numerical Analysis*, 46(2):465–489, 2012.

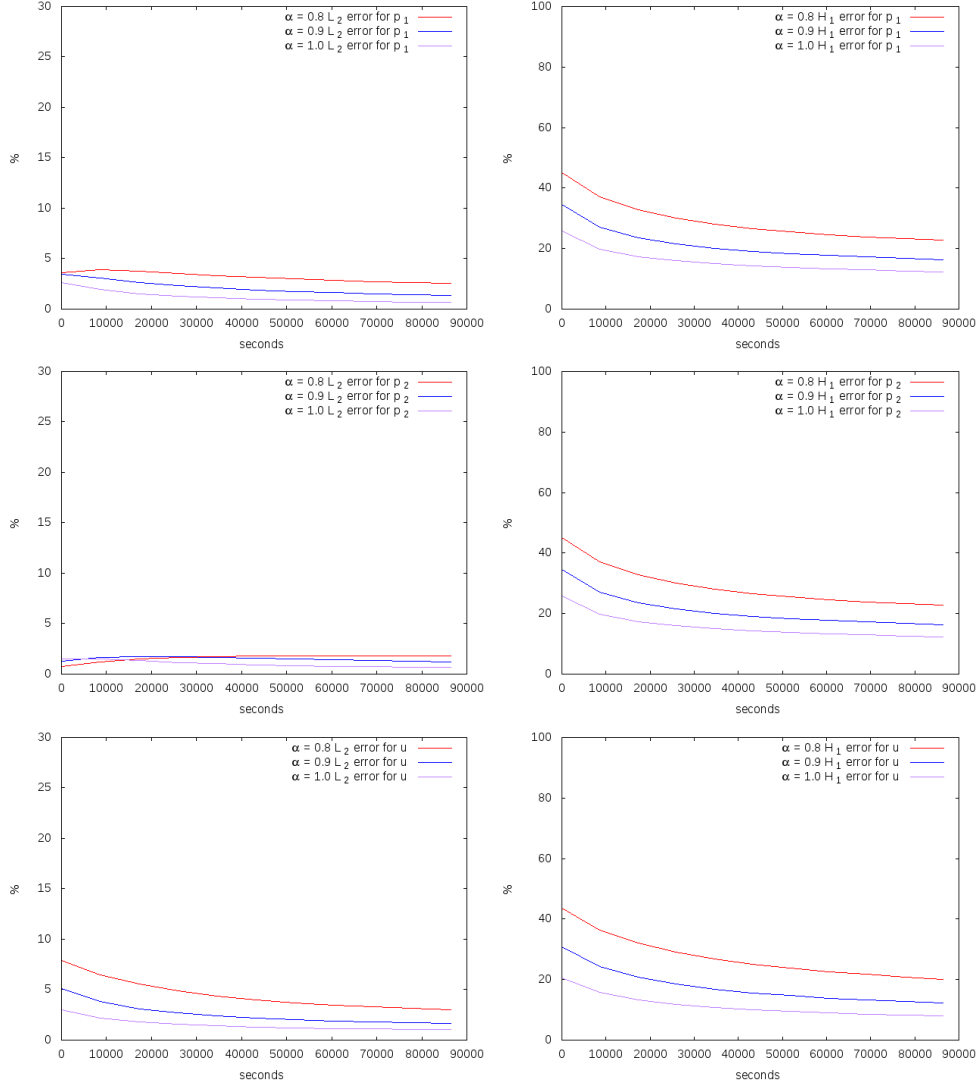


Figure 10: Poroelasticity in multicontinuum media: Relative L_2 error (left) and H_1 (right) errors vs time for different fractional order derivative($\alpha = 0.8, 0.9, 1.0$) for first continuum (first row), second continuum (second row) and displacements (third row) with multiscale basis function 12.

- [17] R. Du, A. A. Alikhanov, and Z.-Z. Sun. Temporal second order difference schemes for the multi-dimensional variable-order time fractional sub-diffusion equations. *Computers & Mathematics with Applications*, 79(10):2952–2972, 2020.
- [18] M. Enelund and P. Olsson. Time domain formulation of the Biot poroelastic theory using fractional calculus. *IFAC Proceedings Volumes*, 39(11):391–396, 2006.
- [19] G.-H. Gao, A. A. Alikhanov, and Z.-Z. Sun. The temporal second order difference schemes based on the interpolation approximation for solving the time multi-term and distributed-order fractional sub-diffusion equations. *Journal of Scientific Computing*, 73(1):93–121, 2017.
- [20] F. Gaspar, J. Gracia, F. Lisbona, and P. Vabishchevich. A stabilized method for a secondary consolidation Biot’s model. *Numerical Methods for Partial Differential Equations: An International*

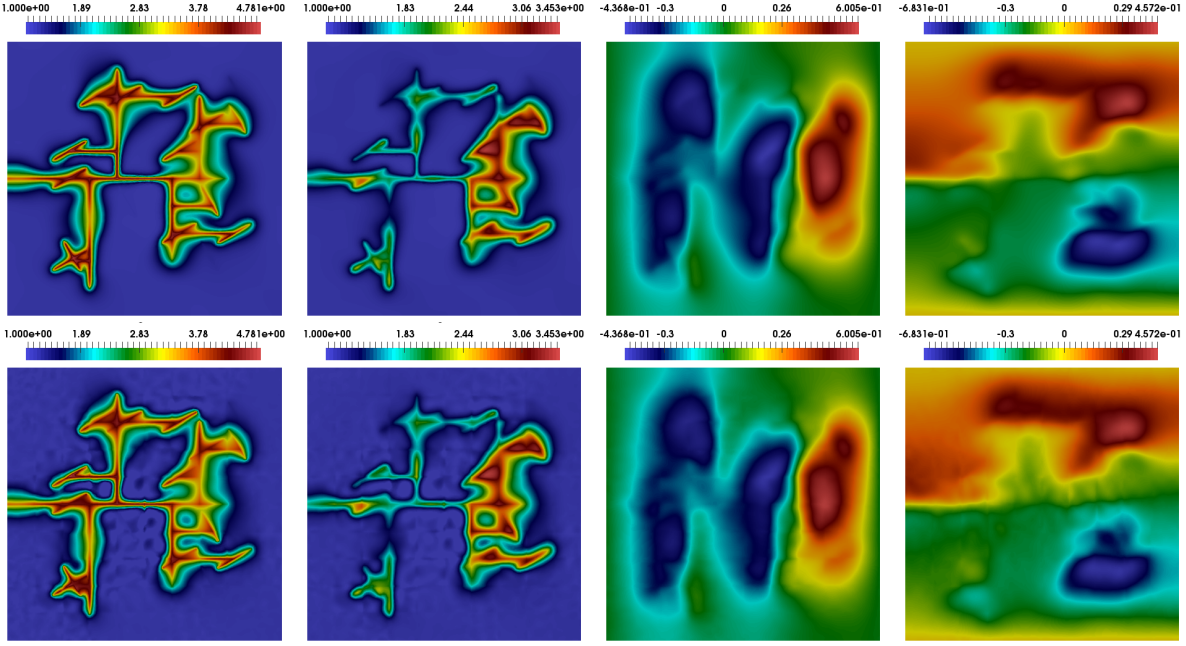


Figure 11: Poroelasticity in multicontinuum media: Distribution of pressure for first and second continuum and displacement along X and Y at final time for fractional order derivative $\alpha = 0.8$ (from left to right). First row: exact solution. Second row: multiscale solution(12 multiscale basis functions).

Journal, 24(1):60–78, 2008.

- [21] U. Gavrilieva, V. Alekseev, and M. Vasilyeva. Numerical homogenization for wave propagation in fractured media. In *AIP Conference Proceedings*, volume 2025, page 100002. AIP Publishing LLC, 2018.
- [22] X.-M. Gu, T.-Z. Huang, C.-C. Ji, B. Carpentieri, and A. A. Alikhanov. Fast iterative method with a second-order implicit difference scheme for time-space fractional convection–diffusion equation. *Journal of Scientific Computing*, 72(3):957–985, 2017.
- [23] H. Hajibeygi, D. Karvounis, and P. Jenny. A hierarchical fracture model for the iterative multiscale finite volume method. *Journal of Computational Physics*, 230(24):8729–8743, 2011.
- [24] O. Iliev, A. Kolesov, and P. Vabishchevich. Numerical solution of plate poroelasticity problems. *Transport in Porous Media*, 115(3):563–580, 2016.
- [25] M. Imran, I. Khan, M. Ahmad, N. Shah, and M. Nazar. Heat and mass transport of differential type fluid with non-integer order time-fractional Caputo derivatives. *Journal of Molecular Liquids*, 229:67–75, 2017.
- [26] M. Karimi-Fard, L. J. Durlofsky, and K. Aziz. An efficient discrete-fracture model applicable for general-purpose reservoir simulators. *SPE journal*, 9(02):227–236, 2004.
- [27] A. E. Kolesov, P. N. Vabishchevich, and M. V. Vasilyeva. Splitting schemes for poroelasticity and thermoelasticity problems. *Computers & Mathematics with Applications*, 67(12):2185–2198, 2014.
- [28] S. H. Lee, M. Lough, , and C. Jensen. Hierarchical modeling of flow in naturally fractured formations with multiple length scales. *Water resources research*, 37(3):443–455, 2001.

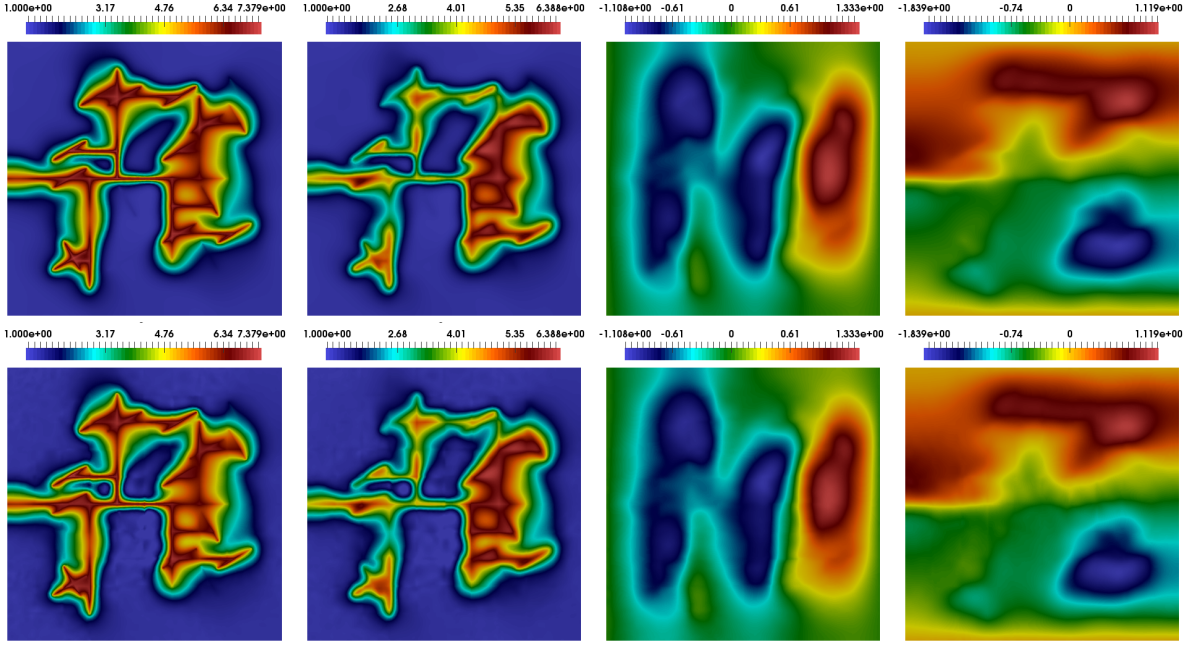


Figure 12: Poroelasticity in multicontinuum media: Distribution of pressure for first and second continuum and displacement along X and Y at final time for fractional order derivative $\alpha = 0.9$ (from left to right). First row: exact solution. Second row: multiscale solution(12 multiscale basis functions).

- [29] L. Li and S. H. Lee. Efficient field-scale simulation for black oil in a naturally fractured reservoir via discrete fracture networks and homogenized media. In *International oil & gas conference and exhibition in China*. OnePetro, 2006.
- [30] L. Li and S. H. Lee. Efficient field-scale simulation of black oil in a naturally fractured reservoir through discrete fracture networks and homogenized media. *SPE Reservoir evaluation & engineering*, 11(04):750–758, 2008.
- [31] F.-J. Liu, Z.-B. Li, S. Zhang, and H.-Y. Liu. He’s fractional derivative for heat conduction in a fractal medium arising in silkworm cocoon hierarchy. *Thermal Science*, 19(4):1155–1159, 2015.
- [32] A. Lorenzi and V. Priimenko. Direct problems for poroelastic waves with fractional derivatives. *SIAM Journal on Mathematical Analysis*, 46(3):1874–1892, 2014.
- [33] M. Mahiuddin, D. Godhani, L. Feng, F. Liu, T. Langrish, and M. Karim. Application of Caputo fractional rheological model to determine the viscoelastic and mechanical properties of fruit and vegetables. *Postharvest Biology and Technology*, 163:111147, 2020.
- [34] A. Meirmanov. *Mathematical models for poroelastic flows*. Springer, 2014.
- [35] S. Mondal. Interactions due to a moving heat source in a thin slim rod under memory-dependent dual-phase lag magneto-thermo-visco-elasticity. *Mechanics of Time-Dependent Materials*, 24(2):233–252, 2020.
- [36] M. Shariyat and R. Mohammadjani. 3D nonlinear variable strain-rate-dependent-order fractional thermoviscoelastic dynamic stress investigation and vibration of thick transversely graded rotating annular plates/discs. *Applied Mathematical Modelling*, 84:287–323, 2020.

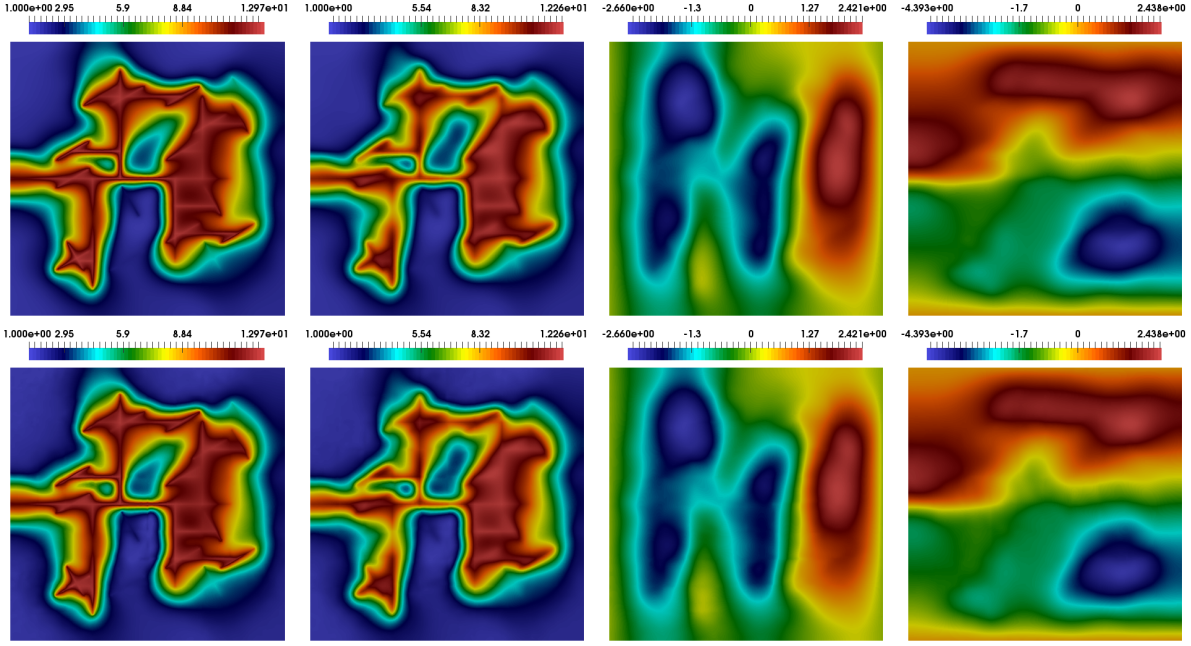


Figure 13: Poroelasticity in multicontinuum media: Distribution of pressure for first and second continuum and displacement along X and Y at final time for fractional order derivative $\alpha = 1.0$ (from left to right). First row: exact solution. Second row: multiscale solution(12 multiscale basis functions).

- [37] A. Talonov and M. Vasilyeva. On numerical homogenization of shale gas transport. *Journal of Computational and Applied Mathematics*, 301:44–52, 2016.
- [38] M. Tene, M. Al Kobaisi, H. Hajibeygi, et al. Algebraic multiscale solver for flow in heterogeneous fractured porous media. In *SPE Reservoir Simulation Symposium*. Society of Petroleum Engineers, 2015.
- [39] M. Tene, M. S. Al Kobaisi, and H. Hajibeygi. Algebraic multiscale method for flow in heterogeneous porous media with embedded discrete fractures (f-ams). *Journal of Computational Physics*, 321:819–845, 2016.
- [40] A. Tyrylgina, M. Vasilyeva, D. Spiridonov, and E. T. Chung. Generalized multiscale finite element method for the poroelasticity problem in multicontinuum media. *Journal of Computational and Applied Mathematics*, 374:112783, 2020.
- [41] V. Vasil'ev and A. Kardashevsky. Iterative identification of the diffusion coefficient in an initial boundary value problem for the subdiffusion equation. *Journal of Applied and Industrial Mathematics*, 15(2):343–354, 2021.
- [42] M. Vasilyeva, E. T. Chung, S. W. Cheung, Y. Wang, and G. Prokopenko. Nonlocal multicontinuum upscaling for multicontinuum flow problems in fractured porous media. *Journal of Computational and Applied Mathematics*, 355:258–267, 2019.
- [43] M. Vasilyeva, E. T. Chung, Y. Efendiev, and J. Kim. Constrained energy minimization based upscaling for coupled flow and mechanics. *Journal of Computational Physics*, 376:660–674, 2019.
- [44] M. Vasilyeva, E. T. Chung, W. T. Leung, and V. Alekseev. Nonlocal multicontinuum (NLMC) upscaling of mixed dimensional coupled flow problem for embedded and discrete fracture models. *GEM-International Journal on Geomathematics*, 10(1):1–23, 2019.

- [45] J. Yao, Z. Huang, Y. Li, C. Wang, X. Lv, et al. Discrete fracture-vug network model for modeling fluid flow in fractured vuggy porous media. In *International oil and gas conference and exhibition in China*. Society of Petroleum Engineers, 2010.
- [46] M. A. Zaky, A. S. Hendy, A. A. Alikhanov, and V. G. Pimenov. Numerical analysis of multi-term time-fractional nonlinear subdiffusion equations with time delay: What could possibly go wrong? *Communications in Nonlinear Science and Numerical Simulation*, 96:105672, 2021.